Distribution and fate of ^{129}I in the seabed sediment off Fukushima

Shigeyoshi Otosaka [a,*], Yuhi Satoh [b], Takashi Suzuki [a], Jun Kuwabara [c], and Takahiro Nakanishi [d]

[a] Research Group for Environmental Sciences, Nuclear Science and Engineering Center, Japan Atomic Energy Agency, 2-4 Shirakata, Tokai, Ibaraki 319-1195, Japan

[b] Department of Radioecology, Institute for Environmental Sciences, 1-7 Ienomae, Obuchi, Rokkasho, Aomori 039-3212, Japan

[c] AMS Management Section, Aomori Research and Development Center, Japan Atomic Energy Agency, 4-24 Minatomachi, Mutsu, Aomori 035-0064, Japan

[d] Fukushima Environmental Safety Center, Japan Atomic Energy Agency, 10-2 Fukasaku, Miharu, Fukushima 963-7700, Japan

* Corresponding author: otosaka.shigeyoshi@jaea.go.jp

Keywords

Fukushima Daiichi Nuclear Power Plant, radioiodine, seabed sediment, sinking particles, coastal environment

Highlights

- Concentration of ^{129}I in seabed sediment off Fukushima is reported for the first time
- Deposition of the FDNPP accident-derived ^{129}I to the seafloor was 0.36 ± 0.13 GBq
- Until October 2013, ^{129}I activity in sediment increased in the shelf-edge region
- Remobilization of ^{129}I near the seafloor likely affected the sequential accumulation
- The accident-derived ^{129}I is considered to negligibly affect the benthic ecosystem

Abstract

In this study, seabed sediment was collected from 26 stations located within 160 km from the Fukushima Dai-ichi Nuclear Power Plant (FDNPP) during the 2 years which followed the FDNPP accident of March 2011 and the concentrations of ^{129}I and ^{137}Cs were measured. By comparing the distribution of these two radionuclides with respect to their different geochemical behaviors in the environment, the transport of accident-derived radionuclides near the seafloor is discussed. The concentration of ^{129}I in seabed sediment recovered from offshore Fukushima in 2011 ranged between 0.02 and 0.45 mBq kg^{-1}, with $^{129}I/^{137}Cs$ activity ratios of $(1.9 \pm 0.5) \times 10^{-6}$ Bq Bq^{-1}. The initial deposition of ^{129}I to the seafloor in the study area was 0.36 ± 0.13 GBq, and the general distribution of sedimentary ^{129}I was established within 6 months after the accident. Although iodine is a biophilic element, the accident-derived ^{129}I negligibly affects the benthic ecosystem. Until October 2013, a slight increase in activity of ^{129}I in the surface sediment along the shelf-edge region (bottom depth: 200-400 m) was observed, despite that such a trend was not observed for ^{137}Cs. The preferential increase of the ^{129}I concentrations in the shelf-edge sediments was presumed to be affected by the re-deposition in the shelf-edge sediments of ^{129}I desorbed from the contaminated coastal sediment. The results obtained from this study indicate that $^{129}I/^{137}Cs$ in marine particles is a useful indicator for tracking the secondary transport of accident-derived materials, particularly biophilic radionuclides, from the coast to offshore areas.

54 1 Introduction

55 After the Fukushima Daiichi Nuclear Power Plant (FDNPP) accident, which occurred on
56 March 11, 2011, large amounts of anthropogenic radionuclides were released into the marine
57 environment (e.g., Buesseler et al., 2017). A majority of the radionuclides were transported
58 through the movement of seawater across a wide area of the North Pacific while some of the
59 radionuclides were deposited on the seabed of the coastal areas of northeastern Japan (e.g.,
60 Otosaka and Kato, 2014). Many studies related to the behavior of radionuclides on the
61 seafloor have focused on radiocesium (particularly ^{137}Cs, half-life = 30.7 years), which emits
62 radiation to the environment. Radiocesium in surface sediments tends to decrease with an
63 apparent half-life of about 2 years, except in the vicinity of the FDNPP and estuaries
64 (Kusakabe et al., 2017; Otosaka, 2017). The rate of decrease in sedimentary radiocesium
65 concentration is less than that of seawater, and it indicates that the radionuclide will remain
66 on the seabed around Fukushima over a longer period (Otosaka, 2017). In addition to
67 seabed sediments, this gradual decrease in the radiocesium activity has been observed in
68 demersal fishes (Wada et al., 2014) and invertebrates (Sohtome et al., 2014). As the
69 decreasing trend in the concentration of radionuclides in the seabed sediment shows the same
70 trend with that in the organisms, sediments are thought to be a source of radionuclides for the
71 ecosystem near the seafloor (Tateda et al., 2015; Wang, 2016). However, the transfer
72 process of the radionuclides from sediments to the benthic ecosystem has not previously been
73 detailed.

74 Besides radiocesium, several nuclear fission products were released into the environment
75 as a result of the accident. Radioiodine is a fission product with a strong affinity for organic
76 matter as well as a high bioavailability (e.g., Santschi and Schwehr, 2004). Hence, ^{131}I
77 (half-life = 8 days), for example, is known to be particularly important for evaluating
78 short-term radiation exposure during radiation accidents (e.g., UNSCEAR, 2014). In the

79 FDNPP accident, ~151 PBq of ^{131}I has been estimated to have been released into the
80 environment (Katata et al., 2015); however, its activity decreased in the early stages after the
81 accident because of its short half-life. Hence, it is not possible to directly estimate the
82 extent of the impact of ^{131}I on the marine environment in the initial stages of the accident.
83 In addition, radioiodine with a long half-life, ^{129}I (half-life = 1.57×10^7 years), was released
84 into the environment as a result of the accident. Assuming that ^{131}I and ^{129}I were released
85 into the environment at a specific ratio, the transport of ^{131}I in the environment after the
86 accident can potentially be traced. In the land area around FDNPP, the initial distribution of
87 ^{131}I has been reconstructed on the basis of this hypothesis (Miyake et al., 2012; Honda et al.,
88 2015; Muramatsu et al. 2015). In addition, ^{129}I has been detected from the seawater around
89 Fukushima after the FDNPP accident (Hou et al., 2013; Suzuki et al., 2013; Casacuberta et al.,
90 2017). The ^{129}I activity concentrations reportedly increased by about an order of magnitude
91 compared with concentrations before the accident (Suzuki et al., 2013), indicating that even
92 in the marine environment the potential of ^{129}I for tracking accident-derived radioiodine.
93 Generally, the concentration of iodine in the seabed sediments is greater than that in soil
94 on the land (e.g., Muramatsu and Wedepohl, 1998). The major factors related to the
95 accumulation of iodine in the sediment include uptake from brown algae and planktons (e.g.,
96 Shaw, 1959); phytoplanktonic-enzyme-mediated adsorption of iodide (Price and Calvert,
97 1973); microbial accumulation of organo-iodine (Amachi et al., 2005); adsorption of iodate
98 onto oxyhydroxides (Ullman and Aller, 1985); and reduction of iodate via humic substances
99 followed by their adsorption on the seafloor (Francois, 1987; Schlegel et al., 2006). Each of
100 these processes provides strong evidence for the high bioavailability of iodine in the ocean.
101 From these facts, it is crucial to understand the distribution of ^{129}I in the seabed
102 sediments around Fukushima for re-evaluating the effect of the FDNPP accident on the
103 marine environment, especially the benthic ecosystem. In this study, the activity

concentrations of ^{129}I in the sediments and sinking particles around Fukushima in the two years after the FDNPP accident are reported for the first time. Sinking particles are biological and geochemical debris that also transport pollutants to the seafloor, and provide useful information for tracking the migration of particulate radionuclides. In this study, the transport of the accident-derived radionuclides near the seafloor is discussed by comparison of the distributions of ^{129}I and ^{137}Cs, which are considered to exhibit different environmental behaviors.

2 Methods

2.1 Sampling

From August 2011 to September 2013, sediment samples were collected from 26 stations (Table 1, Fig. 1), ranging from 1 to 160 km from the FDNPP, using a multiple corer (Model 5173, RIGO Co. Ltd., Japan) or a GS submarine corer (Model 5174, RIGO Co. Ltd., Japan). In Stations J7, K2, K6, S2 and FS1, sediments were collected two times at intervals of 11-14 months. Sediment samples were cut on board to a thickness of 1-3 cm (Table S1 in supplementary materials), frozen, and brought to the laboratory on land. For Sta. J8, sediment samples collected for about 2 years before the accident (July 2009) were also analyzed in addition to that collected seven months after the accident (October 2011).

Sinking particles collected at Sta. FS1, which is about 100 km offshore of FDNPP, were also analyzed. For the analysis of sinking particles, some of the archived samples collected by Otosaka et al. (2014) were used. Hence, the data for the total mass flux are the same as those reported by Otosaka et al. (2014). In this sediment trap experiment, sinking particles were collected at 26-day intervals, however, to secure a sufficient amount of sample for ^{129}I analysis, samples from three periods were combined and analyzed as those collected between August 2011 and January 2012 due to the low mass flux (Table S2). The mixing ratio of the

129 sample in these periods was adjusted to the ratio of the total mass flux.

130

131 2.2 Chemical and radiochemical analysis

132 The sediment samples were dried at 80 ºC, crushed, passed through a 2-mm sieve, and
133 used for ^{129}I analysis. The activity concentrations of radionuclides in the sediment reported
134 herein represents the radioactivity per kilogram of dry weight of sediment.

135 The analysis of ^{129}I in the sediment was carried out according to that reported by
136 Muramatsu et al. (2008). Briefly, ~2 g of dried sediment samples was added to 2~4 mg of
137 an iodine carrier, heated at 1000°C for 20 min in a stream of oxygen in a quartz tube (25 mm
138 ID × 635 mm length), and the volatilized iodine was collected in a receiving solution,
139 comprised of a mixture of tetraethyl ammonium hydroxide (1%) and sodium sulfite (0.1%).
140 Iodine in the receiving solution was extracted in chloroform, and molecular iodine (I_2) in the
141 organic phase was back extracted into an aqueous phase (sodium sulfite) as iodide (I^-), and
142 silver nitrate was added to this aqueous solution to obtain silver iodide. The obtained silver
143 iodide was pressed in a target and the $^{129}I/^{127}I$ isotopic ratio was measured with a Tandetron
144 accelerator mass spectrometer (JAEA-AMS-MUTSU) at the JAEA Aomori Research and
145 Development Center. The concentration of ^{129}I in the sample was calculated from the
146 $^{129}I/^{127}I$ isotope ratio, the amount of carrier, the amount of stable iodine (^{127}I) in the sample,
147 and the amount of sample used for the analysis.

148 For ^{127}I analysis, a 7-100 mg sediment sample was combusted in the same manner as that
149 carried out in the ^{129}I analysis without the addition of the iodine carrier, and the concentration
150 of ^{127}I in the receiving solution was measured by cathodic stripping voltammetry using the
151 method reported by Wong and Zheng (1992). A Metrohm 797VA voltammetric stand
152 (Metrohm AG, Switzerland) with a hanging mercury drop electrode (Multi-Mode Electrode
153 pro, Metrohm AG, Switzerland) was used for the measurement of ^{127}I. The results of ^{127}I

154 measurement include a relative uncertainty of 0.4-19% (7% on average).

155 A standard reference material NIST SRM 3230 (National Institute of Standard and
156 Technology, USA) with a $^{129}I/^{127}I = (9.85 \pm 0.12) \times 10^{-13}$ was used for the standardization of
157 the $^{129}I/^{127}I$ isotopic ratios. The procedural background of $^{129}I/^{127}I$ (based on the
158 measurement of iodide carrier) was $(2.37 \pm 0.34) \times 10^{-13}$, which was 0.5-9.4% (2.7% on
159 average) of the $^{129}I/^{127}I$ signal of sediment samples. The relative error for the ^{129}I
160 concentration measurement was 0.9-5.7% (1.9% on average) of the measured value.

161 Gamma-ray spectrometry using a high purity germanium detector (ORTEC GEM20P4,
162 resolution of 1.7 keV/1.33 MeV and relative efficiencies of 29-31%) was carried out for all
163 samples, and the concentration of ^{137}Cs was calculated from the photopeak counts of 661 keV.
164 For gamma-ray spectrometry, 40-100 g of dry sediments was used, and detectors were
165 calibrated using a volume radioactivity standard (MX033U8PP, Japan Radioisotope
166 Association). Under our analytical conditions (~200000 s counting), the lowest amount of
167 ^{137}Cs that could be determined in a sediment sample was ~27 mBq, corresponding to ~0.4 Bq
168 kg^{-1}.

169 The activities of ^{129}I and ^{137}Cs in the sediment and sinking particles reported herein may
170 also include those originating from global fallout and nuclear fuel reprocessing plants in
171 addition to those observed as a result of the FDNPP accident. However, to investigate the
172 mixing of the radionuclides from different sources, the correction of such “pre-accident”
173 sources is not made for ^{129}I and ^{137}Cs.

174

175 2.3 Suspension experiment

176 To understand the adsorption/desorption characteristics of ^{129}I between the sediment and
177 seawater, a suspension experiment was carried out. In the experiment, sediment samples
178 collected from Stations NP0 (bottom depth: 18 m) and N03 (302 m) were selected as

representatives for the vicinity of FDNPP (sand with low organic matter) and a shelf-edge area (fine sand with high organic matter), respectively.

In this experiment, ~2 kg (in wet weight) of the sediment was suspended in 20 L of artificial seawater and allowed to settle for 70 days with aeration. Before suspension and immediately after the sampling, pore water in the sediment was removed as much as possible by centrifugation (4400 g, 5 min). The water phase was sampled after 0.125, 7, 14, 21, 35, 29 and 70 days from the suspension, filtered through a glass fiber filter (Whatman, GF/F), and the concentrations of ^{129}I and ^{127}I in the water were measured by the method reported by Suzuki et al. (2008). The experiment was performed in duplicate.

As the water samples for ^{129}I measurement at each time step (1L each) were collected from the same system, the sediment to water ratio varied from 1:10 to 1:6. This change in the solid-liquid ratio is expected to lead to an overestimation of the concentration of ^{129}I in the aqueous phase ~1.6 times at the end of the experiment. However, the correction for the concentration was not performed because this experiment was carried out to compare the adsorption/desorption characteristics depending on sediment properties rather than to quantitatively determine the adsorption/desorption rate.

3 Results

3.1 Distribution of ^{129}I and ^{137}Cs in the surface sediment

Figure 2 shows the distributions of the activity concentrations of ^{129}I and ^{137}Cs in the surface (a 0-1 cm or a 0-3 cm layer) sediment. Although the sediment samples in this study were conducted from 2011 to 2013, the results are shown together for all observation dates to reveal the general distribution characteristics. The highest ^{129}I concentration of 0.952 mBq kg^{-1} was observed in January 2013 at Sta. K2 (bottom depth of 272 m), which was located 158 km south of FDNPP. At observation point J8, the concentration of ^{129}I in surface

sediment in October 2011 was 0.189 mBq kg^{-1}. As the concentration at Sta. J8 before the accident (July 2009) was 0.08 mBq kg^{-1}, the concentration of ^{129}I in the surface sediment at Sta. J8 was more than doubled as a result of the accident. At Sta. J8, the concentration of ^{137}Cs was 98.8 Bq kg^{-1} in 2011; this concentration was more than 200 times the value before the accident (<0.4 Bq kg^{-1}) (Table S1). These results revealed that the effect of ^{129}I on the seafloor caused by the FDNPP accident was less than ^{137}Cs. Relatively, high concentrations of ^{129}I and ^{137}Cs were observed in the vicinity of and to the south of FDNPP. Especially in 2011, $^{129}I/^{137}Cs$ ratio exhibited a proportional relationship (Fig. 3), and the relationship between ^{129}I and ^{137}Cs concentrations was expressed by the following equation (1).

$$[^{129}I] = 0.0019 \times [^{137}Cs] + 0.035 \quad (1)$$

where, $[^{129}I]$ and $[^{137}Cs]$ are ^{129}I concentration (mBq kg^{-1}) and ^{137}Cs concentration (Bq kg^{-1}) in surface sediment, respectively. Although the data of sinking particles were not included in Eq. (1), the relationship between the concentrations of ^{129}I and ^{137}Cs in the sinking particles in 2011 is also in approximate agreement with the regression line (Fig. 3).

The ^{129}I concentration did not show a significant relationship with the ^{127}I concentration ($r < 0.20$) (Table S1). As a strong positive correlation was observed between ^{127}I and the organic matter content ($r = 0.94$, $n = 31$, data calculated for the core-top sediments of all stations including the revisit observations), ^{127}I was considered to be bound to organic matter. In contrast, the low correlation between ^{129}I and ^{127}I revealed the unsteady supply of ^{129}I to the seafloor at a shorter timescale less than that for the circulation of organic matter. Generally, the $^{129}I/^{137}Cs$ in the surface sediment increased from 2011 to 2013. Such a high $^{129}I/^{137}Cs$ ratio after 2012 was not observed near the FDNPP, while it was remarkable in the area that is at a certain distance (i.e. 100–160 km) away from FDNPP (Fig. 4a). However,

even at areas more than 80 km away from FDNPP, a high $^{129}I/^{137}Cs$ ratio was not observed at stations with seafloor depths less than 100 m, such as Sta. S2 (93 m depth, $^{129}I/^{137}Cs$ = 0.0026 mBq Bq^{-1}) and J11 (84 m depth, $^{129}I/^{137}Cs$ = 0.0012 mBq Bq^{-1}), and a high $^{129}I/^{137}Cs$ ratio was observed in the shelf edge area (bottom depth = 200-400 m) (Fig. 4b).

In addition, the increased $^{129}I/^{137}Cs$ ratio was observed in the seabed sediments in offshore stations around a depth of 1000 m. In 2011, the $^{129}I/^{137}Cs$ ratio in the offshore area was slightly greater than that in the coastal waters, and the extent of the $^{129}I/^{137}Cs$ increase was less than that in the shelf-edge areas.

3.2 Vertical change in ^{129}I and ^{137}Cs activity concentrations

Figure 5 shows the vertical distributions of concentrations of ^{129}I and ^{137}Cs in sediments at six stations. Excluding that observed in Sta. NP0, a high radionuclide concentration was observed in the surface layer, which generally decreased with increasing depth. At Sta. NP0, which is located about 2 km from the FDNPP, a relatively high radionuclide concentration was observed in the deep sedimentary layer; these radionuclides are thought to have accumulated immediately after the accident. At other stations where the bottom depth was greater than 100 m, the radionuclides accumulated in the upper 10 cm of the sediment. There was little difference in general characteristics of the vertical distribution between ^{129}I and ^{137}Cs. However, at the offshore stations with low radionuclide activities, $^{129}I/^{137}Cs$ was greater than those in coastal areas, and the ratio increased with increasing sediment depth. In other words, sediments that had experienced a greater effect as a result of the FDNPP accident exhibit lower $^{129}I/^{137}Cs$ ratios.

The $^{129}I/^{137}Cs$ ratio in the surface sediment at Sta. J7 increased to approximately two times in 2013 (0.01 mBq Bq^{-1}) compared to that in 2011 (0.0046 mBq Bq^{-1}). The concentration of ^{137}Cs in this layer was 57-62 Bq kg^{-1}, which was 60 times greater than the

averaged ^{137}Cs concentration before the accident in this area (0.87 ± 0.41 Bq kg^{-1}: Kusakabe, 2013). This result indicated that sediments in this station had been strongly affected by the FDNPP accident. In addition, this result suggested that particles with a relatively high ^{129}I concentration had accumulated near the sediment surface in the period between the two observation days. Although the extent of the accumulation was small, the preferential accumulation of ^{129}I in the surface sediments was also observed at Sta. NP3 in the semi-offshore area (117 m depth) and Sta. FS1 in the hemipelagic area (992 m depth).

3.3 ^{129}I and ^{137}Cs in sinking particles

Figure 6 shows the temporal changes in the total mass flux and activity concentration of ^{129}I and ^{137}Cs in sinking particles observed at Sta. FS1. As the total mass flux and ^{137}Cs concentration have been reported in the study by Otosaka et al. (2014), only their main features have been briefly described. The total mass flux was ~400 mg m^{-2} d^{-1} from August to December 2011, and then two maxima were observed in January-March 2012 and in May-June 2012. Contrary to the total mass flux, a high concentration of ^{137}Cs in the sinking particles of 184-243 Bq kg^{-1} from August 2011 to January 2012 was observed. After January 2012 with increasing mass flux, the ^{137}Cs concentration decreased to 41-85 Bq kg^{-1}.

The concentrations of ^{129}I in sinking particles were ~0.6 mBq kg^{-1} in 2011 and then decreased to 0.2-0.3 mBq kg^{-1} in 2012. The concentrations of ^{129}I and ^{137}Cs exhibited similar temporal changes, but the variation of the ^{129}I concentration was less than that of the ^{137}Cs concentration. Hence, the ^{129}I/^{137}Cs ratio is greater in 2012, showing a maximum in February 2012 with the observation of the maximum total mass flux. Subsequently, the ^{129}I/^{137}Cs for the sinking particles decreased, but it remained at a higher level compared with that in 2011 until June 2012 when the observation was terminated.

279

280 3.4 Suspension experiment

281 During the suspension experiment, the concentration of ^{129}I in the aqueous phase varied
282 between 0.03 and 0.63 μBq L^{-1} for Sta. NP0 and between 0.005 and 0.054 μBq L^{-1} for Sta
283 N03 (Fig. 7). Both systems exhibited the lowest concentration immediately (3 h) after the
284 suspension and the highest concentration after 7 days. The transfer rate of ^{129}I from the
285 sediment to the aqueous phases on day 7 was ~3% for Sta. NP0 and ~1% for Sta. N03. At
286 the nearshore station NP0 in the vicinity of FDNPP, the ^{129}I concentration was almost
287 constant from day 7 to day 72. On the other hand, at Sta. N03 in the shelf-edge area, the
288 concentration of ^{129}I in the aqueous phase decreased at a rate of about 0.03 ± 0.01 day^{-1} from
289 day 7 to day 49, and this concentration remained constant until day 72.

290

291 4 Discussion

292 4.1 Effect of accident-derived ^{129}I on the seabed

293 The regression line between the ^{129}I and ^{137}Cs concentrations in 2011 showed an
294 intercept (0.035 ± 0.024 mBq kg^{-1}, Fig. 3). The concentration of ^{137}Cs in the sediment off
295 Fukushima (<30 km from the coast) in 2010 is reported to be 0.87 ± 0.41 Bq kg^{-1} (Kusakabe
296 et al., 2013). The pre-accident ^{137}Cs concentration is extremely less than the variation range
297 of ^{137}Cs in Fig. 3; hence, almost all of the ^{137}Cs observed from the sediment originates from
298 FDNPP. Accordingly, the intercept in Fig. 3 can be considered as the concentration of ^{129}I
299 in the sediment before the FDNPP accident. The global fallout as a result of the
300 atmospheric nuclear weapon tests and nuclear facility operations, especially nuclear fuel
301 reprocessing plants, can be considered as the major sources of ^{129}I to the marine environment
302 before the FDNPP accident (e.g., Snyder et al., 2010).

303 The concentration of ^{129}I in the sediment collected from Sta. J8, which is located

offshore of the spent nuclear fuel reprocessing facility in Tokai-mura, before the accident was 0.08 mBq kg^{-1}. A slightly higher ^{129}I concentration has been reported in the areas around this facility (e.g., Muramatsu et al., 2008). The concentration of ^{129}I concentration in the surface sediment collected from Sta. J8 is slightly greater than the average ^{29}I concentration for the sediments collected from the surrounding sea area (i.e., the intercept in Fig. 3: 0.035 ± 0.024 mBq kg^{-1}).

Although the ^{129}I concentration before the accident apparently changed depending on the sediment characteristics, assuming that the concentration of ^{129}I in the sediment before the FDNPP accident was 0.035 mBq kg^{-1}, the contribution of accident-derived ^{129}I in the surface sediment in 2011 was estimated to be 19% (Sta. K6) to 93% (Sta. J6). The mean ^{129}I contribution values for the coastal (depth <200 m), shelf-edge (water depth 200-400 m), and offshore (water depth 400-1000 m) regions in 2011 are 87% (n = 7), 71% (n = 4), and 81% (n = 6), respectively. This result indicated that the majority of the observed ^{129}I in the sediment was released from FDNPP. From these results, ^{129}I and ^{137}Cs, which determine the slope of regression line in Fig. 3, can be considered to originate from FDNPP.

The initial distribution of radiocesium in sediments around Fukushima has been suggested to be established by the adsorption of dissolved radiocesium in contaminated water onto the seabed (Otosaka and Kato, 2014; Misumi et al., 2014). In addition, the degree of the initial deposition of radiocesium on surface sediments varies with various sediment properties, including particle size (Ambe et al., 2014) and organic matter content (Ono et al., 2015). The result that the $^{129}I/^{137}Cs$ in the surface sediment in 2011 generally remains within a certain range revealed similar characteristics for ^{129}I and ^{137}Cs in terms of the initial deposition on the sediment.

In the region around Fukushima, the maximum radionuclide concentration in seawater was observed on April 6, 2011 (Oikawa et al., 2013). As mentioned above, the main

deposition of the radionuclides to the seafloor was also presumed to occur around this time. In the early period after the FDNPP accident, ^{137}Cs concentrations exceeding 1000 Bq kg^{-1} were detected from the surface sediments (e.g., Otosaka, 2017). By the application of a ^{137}Cs concentration of 1000 Bq kg^{-1} in Eq. (1), the calculated concentration of ^{129}I in this area increased to ~2 mBq kg^{-1}. In addition, the initial deposition of ^{137}Cs on the seafloor in the area where the majority of ^{137}Cs was deposited (35.5-38.5°N, 140.5-142.5°E) as of October 2011 has been estimated to be 0.19 ± 0.05 PBq (Otosaka and Kato, 2014). As the slope of the regression line in Fig. 3 (0.0019 ± 0.0005) can be regarded as the activity ratio between ^{129}I and ^{137}Cs (^{129}I/^{137}Cs, in mBq Bq^{-1}) deposited on sediment after the FDNPP accident, by multiplying ^{129}I/^{137}Cs by the total ^{137}Cs amount, the total amount of ^{129}I in 2011 in the area can be estimated as 0.36 ± 0.13 GBq.

Among the radioiodine released by the FDNPP accident, ^{131}I is particularly important for evaluating the initial radiation dose. The atomic ratio of ^{131}I to ^{129}I (^{131}I/^{129}I) in the environment after FDNPP has been reported as 3.2 × 10^{-2} on March 15, 2011 (Miyake et al., 2012). Considering radioactive decay, the ^{131}I/^{129}I atomic ratio was 4.7 × 10^{-3} and the activity ratio was 3.4 × 10^{3} (Bq mBq^{-1}) on April 6, 2011. By multiplying the ^{131}I/^{129}I activity ratio by the maximum ^{129}I concentration in the sediment (2 mBq kg^{-1}), the concentration of ^{131}I in the surface sediment near Fukushima increased to ~7 × 10^{3} Bq kg^{-1} at maximum.

As an example of the approximate radiation dose assessment, if ^{131}I in the contaminated sediment were to decrease by radioactive decay, and furthermore, 100 g (in wet weight) of fish with the same concentration of ^{131}I as sediments were to be daily ingested for a year, the effective dose would be calculated as ~0.2 mSv year^{-1}. This value is sufficiently low from the viewpoint of dose assessment. In addition, the effective dose of ^{129}I under the same condition was less than 1 × 10^{-7} Sv year^{-1}, which is negligible. Hence, this paper focuses on

tracking the transport of accident-derived radionuclides near the seafloor and not on the dose assessment.

4.2 Tracking the transport of FDNPP accident-derived ^{129}I near the seafloor

4.2.1 Processes affecting the activity of ^{129}I in surface sediments

In the shelf-edge region off Fukushima, from 2011 to 2013, the $^{129}I/^{137}Cs$ in the seabed sediments increased (Figs. 3 and 4). This increase in the $^{129}I/^{137}Cs$ in the shelf-edge sediment was remarkable especially in the sediment surface layer (Fig. 5). Such an increase in $^{129}I/^{137}Cs$ was not observed in the coastal area near the FDNPP. In this study, in 2011 and 2013, observations at the three revisited shelf edge stations, J7 (218 m), K2 (274 m), and K6 (300 m), respectively, were conducted: the ^{129}I concentration at all stations significantly increased. The increase in the inventory of ^{129}I in surface layer (0-1 cm) sediments was 1.4 mBq m^{-2} for Sta. J7, 6.0 mBq m^{-2} for Sta. K2, and 0.92 mBq m^{-2} for Sta. K6. The increase rate of ^{129}I was 2.4 mBq m^{-2} $year^{-1}$ on average (arithmetic mean). Assuming that the shelf edge area (200-400 m depths) of this study is 4.6×10^3 km^2 (Otosaka and Kato, 2014), the concentration of ^{129}I increases by 11 MBq per year in this area. Although this amount is only 3% of the total ^{129}I amount accumulated in the seabed sediments after the FDNPP accident (0.36 GBq), a preferential transport of ^{129}I to the shelf-edge area is suggested to have occurred.

The selective increase in the concentration of ^{129}I at the shelf-edge sediment surface is caused by the (1) preferential supply of ^{129}I from rivers, (2) selective removal of ^{129}I from the water column and its sedimentation, (3) accumulation of ^{129}I on the sediment surface by early diagenesis, and (4) transport of ^{129}I-enriched particles near the seafloor. In the following subsections, the effect of these four processes is discussed.

379 4.2.2 Preferential supply of ^{129}I from rivers

380 The Sendai Bay, which is located in the northern part of the study area in this paper, is
381 affected by the flux of the Abukuma River (Yamashiki et al., 2014; Kakehi et al., 2016),
382 which accounts for the majority of the riverine input in the survey area. According to a
383 survey conducted by Honda et al. (2015) and Matsunaka et al. (2016), the $^{129}I/^{137}Cs$ of the
384 surface soil from the catchment area from these rivers has been reported as 0.0002-0.0006
385 mBq Bq^{-1}. Information regarding the suspended particulate ^{129}I in the Abukuma River is not
386 available, but the $^{129}I/^{137}Cs$ of the suspended particles in the Tomioka River (Fukushima
387 Pref.) is 0.0004-0.0007 mBq Bq^{-1} (Nakanishi, unpublished data), and environmental
388 conditions are similar to those from the soils of Abukuma River catchment areas. The ratio
389 of $^{129}I/^{137}Cs$ that can be supplied from land was one order of magnitude less than the value of
390 the seabed sediments.

391 Among the sampling stations of this study, Sta. J11 and J12 are located in the central part
392 (106 m) and the margin (374 m) of Sendai Bay. Although observations were made at both
393 stations in 2013, an elevated $^{129}I/^{137}Cs$ observed in other stations was not observed, and the
394 ratio was less than that in the other areas. Considering that the stations in the Sendai Bay
395 receive a larger input of fluvial particles with a lower $^{129}I/^{137}Cs$, it is consistent that a low
396 $^{129}I/^{137}Cs$ is observed from the seafloor of these stations.

397 In the first year after the FDNPP accident, the amount of ^{137}Cs deposited on the
398 catchment area where suspended particles can be supplied to the study area is estimated to be
399 2450 TBq (Evrard et al., 2015). In addition, the authors estimated that 1% at maximum of
400 the deposited ^{137}Cs on the catchment flowed in the first one year. Accordingly, in 2011, the
401 inflow rate of ^{137}Cs to the area of this study area has been estimated at 25 TBq $year^{-1}$ at a
402 maximum. By multiplying the ^{137}Cs inflow rate by the above-mentioned $^{129}I/^{137}Cs$ (~0.0007
403 mBq Bq^{-1}), the inflow rate of particulate ^{129}I carried by the rivers was estimated at 18 MBq

404 year^{-1} at a maximum.

405 The amount of ^{129}I supplied from the rivers is similar as that of the secondary
406 accumulated ^{129}I (11 MBq year^{-1}) to the shelf edge area. Considering the fact that most of
407 the particles flowing from the rivers are accumulated at about 10 km from the estuary
408 (Kakehi et al., 2016), ^{129}I may not be sufficiently accumulated over the shelf-edge region
409 greater than 100 km away from the estuary.

410 In addition, the fluvial particles with a low ^{129}I/^{137}Cs activity ratio did not show
411 agreement with the increasing trend of ^{129}I/^{137}Cs in the shelf-edge sediments. The
412 desorption of ^{137}Cs from fluvial particles in the brackish water (Takata et al., 2015; Kakehi et
413 al., 2016) may promote an increase in the ^{129}I/^{137}Cs of suspended particles. However, to
414 explain the ^{129}I/^{137}Cs for the ^{129}I-enriched sediments in the shelf-edge area (> 0.005 mBq
415 Bq^{-1}), more than 80% of ^{137}Cs in the fluvial particles (^{129}I/^{137}Cs = ~0.0007 mBq Bq^{-1}) needs
416 to be desorbed, which is practically difficult.

417

418 4.2.3 Selective removal of ^{129}I from the water column and sedimentation

419 Figure 8 shows the temporal changes of the ^{137}Cs and ^{129}I activity concentrations, as
420 well as ^{129}I/^{137}Cs in the surface seawater in a 30-150 km radius from the FDNPP, which
421 covers the shelf-edge of the study area. The highest concentrations of ^{129}I and ^{137}Cs in the
422 surface seawater were observed in April 2011, followed by a more rapid decrease compared
423 to radioactive decay, and these concentrations remained at a slightly higher level than that
424 before the accident in mid-2012 (Fig. 8a and b). This result indicates that, as of 2012,
425 radionuclides originating from the FDNNP accident are present in the surface seawater of the
426 study area. Although a marginal amount of radionuclides was observed in comparison with
427 that supplied to the ocean immediately after the accident, the continued outflow of polluted
428 water from the FDNPP facilities has been inferred to continue until 2012 as reported by

Kanda (2013).

The $^{129}I/^{137}Cs$ in the seawater has increased over time following an initial decrease of more than two orders of magnitude due to the FDNPP accident; in 2012, the ratio was greater than that before the accident (Fig. 8c). Inside the FDNPP facility in 2012, the removal of radiocesium from the stagnant water in the facility was reinitiated, and part of the processed water was recirculated for cooling the reactor (TEPCO, 2018). With the commencement of the multi-nuclide removal facility operation in March 2013, the removal of ^{129}I from the contaminated water is thought to have been accelerated. Considering this situation, the $^{129}I/^{137}Cs$ ratio of the contaminated water that was recirculating through the plant may have possibly increased until March 2013. In fact, a high $^{129}I/^{137}Cs$ ratio has also been observed from the surface seawater collected in the vicinity of FDNPP from 2012 to 2013 (Casacuberta et al., 2017).

The ^{129}I flux associated with the deposition of "freshly-produced" sedimentary particles derived from biological production in the ocean surface can be simplified below.

$$F_{\text{I-129}} = [^{129}\text{I}]_{\text{SW}} \times CF \times BMF \times f \quad (2)$$

Here, $F_{\text{I-129}}$, $[^{129}\text{I}]_{\text{SW}}$, *CF*, and *BMF* denote the sinking flux of ^{129}I (Bq m^{-2} $year^{-1}$), concentration of ^{129}I in the seawater (μBq L^{-1}), concentration ratio between the seawater and phytoplankton (L kg_{wet}^{-1}), and the mass flux of biogenic particles (the sum of biogenic opal, biogenic carbonate, and organic matter) (kg_{dry} m^{-2} $year^{-1}$), respectively. The representative concentration of ^{129}I in the surface seawater (0.2 μBq L^{-1}: Fig. 8) was taken as the value of $[^{129}\text{I}]_{\text{SW}}$, and the recommended CF value was 800 L kg_{wet}^{-1} (IAEA, 2004). With regards to the *BMF* value, an annual mean value of 0.094 kg_{dry} m^{-2} $year^{-1}$, was calculated from the total particle flux observed for the offshore station FS1 (Table S2) and the concentration of the

biogenic component in each period (Otosaka et al., 2014). *f* is a coefficient obtained by multiplying the wet to the dry weight ratio of the biogenic particles (10: Sladecek and Sladeckova, 1963) and the ratio for the mass accumulation rate of the shelf edge to the offshore (4: Otosaka and Kato, 2014), and which was set as 40. As a condition to apply the *CF*, the concentration of the target element in the living organisms and the ambient seawater needs to be at equilibrium. The actual site was not in equilibrium but in the transition period of ^{129}I from seawater to organisms, $F_{\text{I-129}}$ would be overestimated.

The estimated $F_{\text{I-129}}$ was ~0.6 mBq m^{-2} year^{-1}. Despite the overestimation, the accumulation of ^{129}I in the surface sediments of the shelf margin (2.4 mBq m^{-2} year^{-1}) cannot be explained, indicating that this process does not lead to the accumulation of ^{129}I on the seafloor of the shelf margin.

4.2.4 Accumulation of ^{129}I on the sediment surface by early diagenesis

Iodine in the sediment mainly originates from the organic fraction, which is desorbed as iodide (I^-) because of the decomposition of organic matter under anoxic conditions (e.g., Farrenkopf and Luther III, 2002). In oxidative seawater, an enzyme, e.g., iodide oxidase, which is related to the initial degradation of plankton cells in oxidative seawater, stimulates the oxidation of iodide to molecular iodine (I_2) or hypoiodous acid (HOI^-), which exhibits a high affinity for organic matter (Price and Calvart, 1973). Recent studies have demonstrated that bacteria extracted from marine sediments produce HOI^- with a high efficiency (e.g., Amachi et al., 2005). Some aerobic bacteria have been known to oxidize iodide to I_2 (Gozlan and Margalith, 1973). Consequently, the desorbed iodide can be concentrated on the oxic sediment surface (Kennedy and Elderfield, 1987).

The desorption of ^{137}Cs from the seabed has also been pointed out from the mass balance of ^{137}Cs in the seabed near Fukushima (Otosaka, 2017), the culture experiment of

benthos (Wang et al., 2016), and simulation by an ecosystem model (Tateda et al., 2013; 2015). As described in Section 4.1, the behavior of ^{137}Cs and ^{129}I in sediments is not considerably different, and ^{129}I is considered to be desorbed and diffused in the pore of the sediments. Indeed, from the results obtained from suspension experiments (Fig. 7), a small percentage of ^{129}I migrates from the sedimentary phase to the aqueous phase after several days, regardless of the sediment properties, also indicative of the desorption of ^{129}I from the sediment in this study area.

The accumulation of dissolved matter on the oxic sediment surface is expected to be noticeable in highly redox-sensitive elements such as manganese (Mn). At Sta. J7 where the concentration of ^{129}I in the surface sediment was remarkably high among the stations of this study, the concentration of Mn in the surface sediment was 797 ppm. This value is similar to those in sub-surface layers (1-10 cm; 730 ppm on average), with no evidence for the remarkable enrichment of Mn in the core top. Even in the other shelf-edge stations, the concentration of Mn in the surface sediment was around 400-700 ppm, and no remarkable oxidation layer as observed in the pelagic ocean was observed. From these results, the enrichment of ^{129}I to the shelf-edge sediment surface caused by early diagenesis is not a major process affecting the preferential accumulation of ^{129}I in this region.

4.2.5 Transport of ^{129}I enriched particles

The maximum ^{129}I/^{137}Cs for the sinking particles collected at 100 km offshore of FDNPP was observed in winter (Fig. 6c). In this period, the mass flux sharply increased and this high flux was not caused by the sinking of biogenic particles produced in the surface layer but by the resuspension of surface sediments near the station or lateral transport of coastal sediments (Otosaka et al., 2014). These results indicated that the resuspended particles in seawater may be laterally transported while selectively incorporating ^{129}I into the particles.

504 The nearshore sediments around Fukushima are mainly comprised of medium/coarse sand
505 (Aoyagi and Igarashi, 1999). In the area in which the water depth is less than the nearshore
506 wave base (~30 m), the disturbance of surface sediments can occur during heavy weather
507 (e.g., Otosaka, 2017). Even with the occurrence of resuspension, the extent of horizontal
508 transport of such sandy sediment is limited because of the rapid sinking of sand particles.
509 On the other hand, components dissolved in the pore water of the sandy sediments in the
510 nearshore region can sufficiently diffuse into the overlying water as a result of the
511 disturbance.

512 The desorption of ^{129}I from the sediment to the pore water is also evident from the
513 results obtained by the suspension experiment (Fig. 7). In other words, the nearshore
514 sediment around Fukushima is thought to function as a source of ^{129}I to the seawater on the
515 seabed. Compared with the nearshore station NP0, the median grain size and organic matter
516 content of the shelf-edge station N03 is about half and 3 times, respectively. In the
517 suspension experiment, ^{129}I once desorbed from the sediment of N03 was removed from the
518 water phase at a rate of ~3% per day (probably absorbed on the sedimentary phase) and
519 reached equilibrium in ~40 days. On the other hand, sediments of Sta. NP0 did not exhibit a
520 remarkable adsorption during the experiment for at least 70 days. This difference between
521 the two stations is presumably related to the large specific surface area and high organic
522 matter content of the shelf edge sediment.

523 As mentioned above, iodide-^{129}I which is desorbed from the seabed is mildly oxidized to
524 iodate-^{129}I as a result of biotic and abiotic effects. Concurrently with such a gradual
525 oxidation process, iodate-^{129}I is thought to be reduced to reactive hypoiodous acid by a
526 reaction on the humic substance surface (Francois, 1987; Schlegel et al., 2006) or an enzyme
527 reaction by nitrate reductase present in aerobic organisms (Tsunogai and Sase, 1969). The
528 adsorption of iodate-^{129}I to oxyhydroxides in suspended particles (Ullman and Aller, 1985)

has also been considered to be an effective mechanism to generate ^{129}I-enriched particles near the seafloor.

From these results, a part of ^{129}I in the sediment was desorbed from the sandy nearshore sediment and incorporated into suspended particles comprising high organic matter content, followed by the accumulation of the ^{129}I-enriched suspended particles on shelf-edge sediment surface. Charette et al. (2013) reported that the exchange rate of the coastal seawater around Fukushima after the FDNPP accident was around 30 days. As the value was obtained for surface water, the bottom waters circulate for a longer (months to years) timescale. This is a reasonable timescale for the desorption of ^{129}I from the nearshore region and re-accumulation on the shelf edge sediments.

For FDNPP-derived ^{137}Cs in sediments, more than 80% of the initial deposition has been estimated to occur in coastal areas with a depth less than 100 m. A majority of the ^{129}I deposited in the sediment immediately after the accident (0.36 GBq) can also be presumed to have deposited in the coastal zone. A few percentage of sedimentary ^{129}I in the coastal area are desorbed from the seabed and redeposited in the shelf-edge region, which is sufficient to serve as a source of increased ^{129}I (11 MBq) in the shelf-edge region. This process can most consistently explain the secondary transport of ^{129}I at the shelf area.

5. Conclusion

After the FDNPP accident in March 2011, some of the radioiodine released to the environment was deposited on the seabed. The concentrations of ^{131}I and ^{129}I in sediments were estimated to increase to ~7 kBq kg^{-1} and 0.2 mBq kg^{-1}, respectively. Although iodine is a highly biophilic element, the effective dose by the accident-derived radioiodine was negligible. The initial deposition of ^{129}I to the seafloor was estimated to be 0.36 ± 0.13 GBq.

554 Between 2011 and 2013, ^{129}I was selectively deposited on the surface sediment of the
555 shelf-edge area further away from the FDNPP. The re-deposition of the ^{129}I desorbed from
556 the contaminated coastal sediment to the shelf-edge sediments was presumed to be dominant
557 process affecting the selective accumulation of ^{129}I.

558 Although further discussion is required for verification, the results of this study
559 suggested that $^{129}I/^{137}Cs$ in the seabed sediments and marine particles are useful indicators for
560 evaluating the secondary transport in the coast-offshore systems. In particular, it is expected
561 to be effective for tracking the transport of highly bioavailable radionuclides near the seabed.

562

563 Acknowledgments

564 The authors are grateful to captains, crews and scientists on R/V Tansei-Maru KT-11-27,
565 KT-13-01, R/V Hakuho-Maru KH-11-07 (Univ. of Tokyo/JAMSTEC), R/V Soyo-Maru 1207
566 (Natl. Res. Inst. Fish. Sci., Japan) and R/V Seikai (JAEA) cruises for their assistance in the
567 fieldwork. We are also grateful to H. Narita, Y. Kato, J. Nishikawa (Tokai Univ.), M.
568 Uematsu, H. Obata (Univ. Tokyo), H. Tazoe (Hirosaki Univ.), T. Morita, T. Ono, H.
569 Kaeriyama, D. Ambe (Natl. Res. Inst. Fish. Sci., Japan), Y. Tennichi (KEEA), M. Nakano, S.
570 Kabuto, N. Kinoshita, T. Isozaki, M. Nagaoka, S. Sakamoto, E. Takeuchi, M. Hirasawa, K.
571 Matsumura (JAEA) for their support in field and laboratory works and valuable comments.
572 This research was financially supported by a block grant to Japan Atomic Energy Agency.
573 We thank Dr. S. Hisamatsu and two anonymous reviewers for their insightful and
574 constructive comments on this manuscript.

575

References

Amachi, S., Mishima, Y., Shinoyama, H., Muramatsu, Y., Fujii, T., 2005. Active transport and accumulation of iodide by newly isolated marine bacteria. Appl. Environ. Microbiol. 71, 741-745.

Ambe, D., Kaeriyama, H., Shigenobu, Y., Fujimoto, K., Ono, T., Sawada, H., Saito, H., Miki, S., Setou, T., Morita, T., 2014. Five-minute resolved spatial distribution of radiocesium in sea sediment derived from the Fukushima Dai-ichi Nuclear Power Plant. J. Environ. Radioact. 138, 264-275

Aoyagi, K., Igarashi, C., 1999. On the size distribution of sediments in the coastal sea of Fukushima Prefecture. Bull. Fukushima Pref. Fish. Exp. Sta., 1999, 8, 69-81 (in Japanese).

Buesseler, K., Dai, M., Aoyama, M., Benitez-Nelson, C., Charmasson, S., Higley, K., Maderich, V., Masque, P., Morris, P.J., Oughton, D., Smith, J.N., 2017. Fukushima Daiichi–derived radionuclides in the ocean: Transport, fate, and impacts. Annu. Rev. Mar. Sci. 9, 173–203.

Casacuberta, N., Christl, M., Buesseler, K.O., Lau, Y., Vockenhuber, C., Castrillejo, M., Synal, H.-A., Masqué, P., 2017. Potential releases of ^{129}I, ^{236}U, and Pu isotopes from the Fukushima Dai-ichi Nuclear Power Plants to the ocean from 2013 to 2015. Environ. Sci. Technol. 51, 9826−9835.

Charette, M.A., Breier, C.F., Henderson, P.B., Pike, S.M., Rypina, I.I., Jayne, S.R., and Buesseler, K.O., 2013. Radium-based estimates of cesium isotope transport and total direct ocean discharges from the Fukushima Nuclear Power Plant accident. Biogeosciencs 10, 2159–2167, doi:10.5194/bg-10-2159-2013

Evrard, O., Laceby, J.P., Lepage, H., Onda, Y., Cerdan, O., Ayrault, S., 2015. Radiocesium transfer from hillslopes to the Pacific Ocean after the Fukushima Nuclear Power Plant accident: A review. J. Environ. Radioact. 148, 92-110.

Farrenkopf, A.M., Luther III, G.W., 2002. Iodine chemistry reflects productivity and denitrification in the Arabian Sea: evidence for flux of dissolved species from sediments of western India into the OMZ. Deep Sea Res. II 49, 2303-2318.

Francois, R., 1987. The influence of humic substances on the geochemistry of iodine in nearshore and hemipelagic marine sediments. Geochim. Cosmoshim. Acta 51, 2411-2421.

Gozlan, R.S., Margalith, P., 1973. Iodide oxidation by a marine bacterium. J. Appl. Bact. 36, 407-417.

610 Honda, M., Matsuzaki, H., Miyake, Y., Maejima, Y., 2015. Depth profile and mobility of
611 ^{129}I and ^{137}Cs in soil originating from the Fukushima Dai-ichi Nuclear Power Plant
612 accident. J. Environ. Radioact. 146, 35-43.
613 Hou, X., Povinec, P.P., Zhang, L., Shi, K., Biddulph, D., Chang, C.-C., Fan, Y., Golser, R.,
614 Hou, Y., Ješkovský, M., Jull, A.J.T., Liu, Q., Luo, M., Steier, P., Zhou, W., 2013.
615 Iodine-129 in seawater offshore Fukushima: Distribution, inorganic speciation, sources,
616 and budget. Environ. Sci. Technol. 47, 3091−3098.
617 IAEA (International Atomic Energy Agency), 2004. Sediment Distribution Coefficients and
618 Concentration Factors for Biota in the Marine Environment. IAEA Technical Report
619 Series 422, International Atomic Energy Agency, Vienna, pp. 95.
620 Kanda, J., 2013. Continuing ^{137}Cs release to the sea from the Fukushima Dai-ichi Nuclear
621 Power Plant through 2012. Biogeosciences, 10, 6107–6113.
622 Kaeriyama, H, Ambe, D., Shigenobu, Y., Fujimoto, K., Ono, T., Nakata, K., Morita, T.,
623 Watanabe, T., 2014. ^{134}Cs and ^{137}Cs in seawater around Japan after the Fukushima
624 Daiichi Nuclear Power Plant accident. Oceanogr. Jpn. 23, 127−146 (in Japanese).
625 Kakehi, S., Kaeriyama, H., Ambe, D., Ono, T., Ito, S., Shimizu, Y., Watanabe, T., 2016.
626 Radioactive cesium dynamics derived from hydrographic observations in the Abukuma
627 River estuary, Japan. J. Environ. Radioact. 153, 1-9.
628 Katata, G., Chino, M., Kobayashi, T., Terada, H., Ota, M., Nagai, H., Kajino, M., Draxler, R.,
629 Hort, M.C., Malo, A., Torii, T., Sanada, Y., 2015. Detailed source term estimation of the
630 atmospheric release for the Fukushima Daiichi Nuclear Power Station accident by
631 coupling simulations of an atmospheric dispersion model with an improved deposition
632 scheme and oceanic dispersion model. Atmos. Chem. Phys. 15, 1029–1070.
633 Kennedy, H.A., Elderfield, H., 1987. Iodine diagenesis in pelagic deep-sea sediments.
634 Geochim. Cosmochim. Acta 51, 2489-2504.
635 Kusakabe, M., Oikawa, S., Takata, H., Misonoo, J., 2013. Spatiotemporal distributions of
636 Fukushima-derived radionuclides in nearby marine surface sediments. Biogeosciences
637 10, 5019–5030.
638 Kusakabe, M., Inatomi, N., Takata, H., Ikenoue, T., 2017. Decline in radiocesium in seafloor
639 sediments off Fukushima and nearby prefectures. J. Oceanogr. 73, 529–545.
640 Matsunaka, T., Sasa, K., Sueki, K., Takahashi, T., Satou, Y., Matsumura, M., Kinoshita, N.,
641 Kitagawa, J., Matsuzaki, H., 2016. Pre- and post-accident ^{129}I and ^{137}Cs levels, and
642 ^{129}I/^{137}Cs ratios in soil near the Fukushima Dai-ichi Nuclear Power Plant, Japan. J.
643 Environmen. Radioact. 151, 209-217.

644 Misumi, K., Tsumune, D., Tsubono, T., Tateda, Y., Aoyama, M., Kobayashi, T., Hirose, K.,
645 2014. Factors controlling the spatiotemporal variation of ^{137}Cs in seabed sediment off
646 the Fukushima coast: Implications from numerical simulations. J. Environ. Radioact.
647 136, 218-228.
648 Miyake, Y., Matsuzaki, H., Fujikawa, T., Saito, T., Yamagata, T., Honda, M., Muramatsu, Y.,
649 2012. Isotopic ratio of radioactive iodine (^{129}I/^{131}I) released from Fukushima Daiichi
650 NPP accident. Geochem. J. 46, 327-333.
651 Muramatsu, Y., Wedepohl, K.H., 1998. The distribution of iodine in the earth's crust. Chem.
652 Geol. 147, 201-216.
653 Muramatsu, Y., Takada, Y., Matsuzaki, H., Yoshida, S., 2008. AMS analysis of ^{129}I in
654 Japanese soil samples collected from background areas far from nuclear facilities. Quat.
655 Geochronol. 3, 291–297.
656 Muramatsu, Y., Matsuzaki, H., Toyama, C., Ohno, T., 2015. Analysis of ^{129}I in the soils of
657 Fukushima Prefecture: Preliminary reconstruction of ^{131}I deposition related to the
658 accident at Fukushima Daiichi Nuclear Power Plant (FDNPP). J. Environmen.
659 Radioact. 139, 344-350.
660 Oikawa, S., Takata, H., Watabe, T., Misonoo, J., Kusakabe, M., 2013. Distribution of the
661 Fukushima-derived radionuclides in seawater in the Pacific off the coast of Miyagi,
662 Fukushima, and Ibaraki Prefectures, Japan. Biogeosci, 10, 5031–5047.
663 Ono, T., Ambe, D., Kaeriyama, H., Shigenobu, Y., Fujimoto, K., Sogame, K., Nishiura, N.,
664 Fujikawa, T., Morita, T., Watanabe, T., 2015. Concentration of ^{134}Cs + ^{137}Cs bonded to
665 the organic fraction of sediments offshore Fukushima, Japan. Geochem. J. 49,
666 219-227.
667 Otosaka, S., 2017. Processes affecting long‐term changes in ^{137}Cs concentration in surface
668 sediments off Fukushima. J. Oceanogr. 73, 559–570.
669 Otosaka, S., Kato, Y., 2014. Radiocesium derived from the Fukushima Daiichi Nuclear
670 Power Plant accident in seabed sediments: Initial deposition and inventories. Environ.
671 Sci. Processes Impacts 16, 978-990.
672 Otosaka, S., Nakanishi, T., Suzuki, T., Satoh, Y., Narita, H., 2014. Vertical and lateral
673 transport of particulate radiocesium off Fukushima. Environ. Sci. Technol. 48,
674 12595−12602.
675 Price, N.B., Calvert, S.E., 1973. The geochemistry of iodine in oxidised and reduced recent
676 marine sediments. Geochim. Cosmochim. Acta 37, 2149-2158

677 Santschi, P.H., Schwehr, K.A, 2004. $^{129}I/^{127}I$ as a new environmental tracer or
678 geochronometer for biogeochemical or hydrodynamic processes in the hydrosphere and
679 geosphere: the central role of organo-iodine. Sci Total Environ. 321, 257–271.
680 Schlegel, M.L., Reiller, P., Mercier-Bion, F., Barre, N., Moulin, V., 2006. Molecular
681 environment of iodine in naturally iodinated humic substances: Insight from X-ray
682 absorption spectroscopy. Geochim. Cosmochim. Acta 70, 5536-5551.
683 Shaw, T.I., 1959. The mechanism of iodine accumulation by the brown seaweed, *Laminaria*
684 *digitata* II Respiration and iodide uptake. Proc. Roy. Soc. London 152, 109-117.
685 Snyder, G., Aldahan, A., Possnert, G., 2010. Global distribution and long-term fate of
686 anthropogenic ^{129}I in marine and surface water reservoirs. Geochem. Geophys. Geosyst.
687 11, Q04010, doi:10.1029/2009GC002910.
688 Sohtome, T., Wada, T., Mizuno, T., Nemoto, Y., Igarashi, S., Nishimune, A., Aono, T., Ito, Y.,
689 Kanda, J., Ishimaru, T., 2014. Radiological impact of TEPCO's Fukushima Dai-ichi
690 Nuclear Power Plant accident on invertebrates in the coastal benthic food web. J.
691 Environ. Radioact. 138, 106-115.
692 Sladecek, V., Sladeckova, A., 1963. Relationship between wet weight and dry weight of the
693 periphyton. Limnol. Oceanogr. 8, 309–311.
694 Suzuki, T., Kabuto, S., Amano, H., Togawa, O., 2008. Measurement of iodine-129 in
695 seawater samples collected from the Japan Sea area using accelerator mass
696 spectrometry: Contribution of nuclear fuel reprocessing plants. Quat. Geochronol. 3,
697 268–275.
698 Suzuki, T., Otosaka, S., Kuwabara, J., Kawamura, H., Kobayashi, T., 2013. Iodine-129
699 concentration in seawater near Fukushima before and after the accident at the
700 Fukushima Daiichi Nuclear Power Plant. Biogeosciences 10, 3839–3847.
701 Takata, H., Hasegawa, K., Oikawa, S., Kudo, N., Ikenoue, T., Isono, R., Kusakabe, M., 2015.
702 Remobilization of radiocesium on riverine particles in seawater: The contribution of
703 desorption to the export flux to the marine environment. Mar. Chem. 176, 51–63.
704 Tateda, Y., Tsumune, D., Tsubono, T., 2013. Simulation of radioactive cesium transfer in the
705 southern Fukushima coastal biota using a dynamic food chain transfer model. J. Environ.
706 Radioact. 124, 1-12.
707 Tateda, Y., Tsumune, D., Tsubono, T., Aono, T., Kanda, J., Ishimaru, T., 2015. Radiocesium
708 biokinetics in olive flounder inhabiting the Fukushima accident-affected Pacific coastal
709 waters of eastern Japan. J. Environ. Radioact. 147, 130-141.
710 TEPCO (Tokyo Electric Power Co.), 2018. Contaminated Water Treatment.

711 http://www.tepco.co.jp/en/ decommision/planaction/alps/index-e.html
712 Tsunogai, S., Sase, T., 1969. Formation of iodide-iodine in the ocean. Deep-Sea Res. 16,
713 489-496.
714 Ullman, W.J., Aller, R.C., 1985. The geochemistry of iodine in near-shore carbonate
715 sediments. Geochim. Cosmochim. Acta 49, 967-978.
716 UNSCEAR (United Nations Scientific Committee on the Effects of Atomic Radiation) 2014.
717 UNSCEAR 2013 Report: Sources, Effects and Risks of Ionizing Radiation, Vol. I,
718 Report to the General Assembly (A/68/46), Annex A: Levels and effects of radiation
719 exposure due to the nuclear accident after the 2011 great east-Japan earthquake and
720 tsunami. United Nations, New York, pp.311.
721 Wada, T., Nemoto, Y., Shimamura, S., Fujita, T., Mizuno, Sohtome, T., Kamiyama, K., Morita,
722 T., Igarashi, S., 2014. Effects of the nuclear disaster on marine products in Fukushima.
723 J. Environ. Radioact. 124, 246-254.
724 Wang, C., Baumann, Z., Madigan, D.J., Fisher, N.S., 2016. Contaminated marine sediments
725 as a source of cesium radioisotopes for benthic fauna near Fukushima. Environ. Sci.
726 Technol. 50, 10448-10455.
727 Wong, G.T.F., Zheng, L.-S., 1992. Chemical removal of oxygen with sulfite for the
728 polarographic or voltammetric determination of iodate or iodide in seawater. Mar. Chem.
729 38, 109-116.
730 Yamashiki, Y., Onda, Y., Smith, H.G., Blake, W.H., Wakahara, T., Igarashi, Y., Matsuura, Y.,
731 Yoshimura, K., 2014. Initial flux of sediment-associated radiocesium to the ocean from
732 the largest river impacted by Fukushima Daiichi Nuclear Power Plant. Sci. Rep. 4,
733 3714, doi: 10.1038/srep03714.
734

735 Table 1 Stations for sediment coring

Station	Latitude (°N)	Longitude (°E)	Depth (m)	Distance* (km)	Sampling date (year/month/day)
J6	36.766	141.405	499	80	2011/10/31
J7	36.800	141.250	218	72	2011/10/31; 2013/1/13
J8	36.284	141.117	709	127	2009/7/18; 2011/10/31
J9	36.283	140.900	223	127	2011/10/31
K1	36.000	140.883	102	159	2011/11/1
K2	36.000	141.017	272	158	2011/11/1; 2013/1/13
K3	36.000	141.167	597	158	2011/11/1
K6	37.334	141.668	300	57	2011/10/29; 2013/1/13
K7	37.334	141.834	501	71	2011/10/29
K8	37.317	142.192	1053	103	2011/10/29
K9	36.998	141.300	158	53	2011/10/31
S2	36.590	140.731	35	96	2011/10/27; 2013/2/14
S3	36.679	140.788	47	85	2011/10/27
S4	36.768	140.788	26	76	2011/10/27
S5	36.768	140.899	75	74	2011/10/27
S8	36.502	140.788	75	105	2011/10/27
FS1**	37.333	142.167	992	100	2011/8/2; 2012/7/20
FS5	36.000	141.333	1175	160	2011/8/3
J11	38.088	141.485	121	84	2013/1/14
J12	38.000	142.000	374	106	2013/1/16
N03	36.500	141.000	302	102	2013/9/9
NP3	37.410	141.297	117	23	2013/9/10
NP1	37.415	141.175	54	12	2013/9/10
NP2	37.417	141.102	28	6	2013/9/11
NP0	37.422	141.060	18	2	2013/9/11
NPE2	37.502	141.087	22	10	2013/9/11

736 * Distance from FDNPP
737 ** Sinking particles were also collected with sediment trap
738
739

Figure Captions

Fig. 1 Sampling locations. Open and filled circles indicate stations observed in 2011 and 2012/2013, respectively. Open squares indicate stations observed in both sampling periods.

Fig. 2 Distribution of (a) ^{129}I and (b) ^{137}Cs in the surface sediment. Activities of ^{137}Cs are decay-corrected to March 11, 2011.

Fig. 3 Relationship between the activity concentration of ^{129}I and ^{137}Cs in the surface sediment and sinking particles. Dotted line indicates the regression line based on the sediment data sampled in 2011.

Fig. 4 (a) $^{129}I/^{137}Cs$ in the surface sediment relative to the distance from FDNPP, (b) $^{129}I/^{137}Cs$ in the surface sediment relative to the bottom depth. Shaded area in Fig. (b) represents shelf edge (water depth 200-400 m) region.

Fig. 5 Vertical distribution of the concentration of ^{129}I (left, mBq kg^{-1}), concentration of ^{137}Cs (center, Bq kg^{-1}), and activity ratio of $^{129}I/^{137}Cs$ (right, mBq $Bq^{-1} \times 10^3$) in sediment. Filled and open circles indicate data observed in 2011 and 2012/2013, respectively. Arrows in panels for Sta. J8 indicate activity concentration in surface (0-1 cm) sediment observed before the FDNPP accident (July 2009).

Fig. 6 Time series of the (a) total mass flux, (b) ^{129}I and ^{137}Cs activity concentrations, and (c) $^{129}I/^{137}Cs$ activity ratio for the sinking particles collected from an offshore station, FS1. Dotted line in Fig. (a) indicates original data before mixing of the sample.

Fig. 7 Results obtained from the suspension experiment. Two stations were selected for the experiment; (a) about 2 km offshore of FDNPP (Sta NP0), and (b) shelf edge at 102 km southeast of FDNPP (Sta. N03). Error bar shows the range of the duplicate experiment.

Fig. 8 Time series of the activity concentrations of (a) ^{137}Cs and (b) ^{129}I in the surface seawater. Figure (c) shows the activity ratio of $^{129}I/^{137}Cs$. The $^{129}I/^{137}Cs$ ratio from March to May 2011 was calculated from values reported by Tokyo Electric Power Co. and the Ministry of Education, Culture, Sports, Science and Technology. As the radioiodine concentration was reported for ^{131}I, the ^{131}I activity was converted to this ^{129}I activity by the method described in section 4.1. The ^{131}I and ^{137}Cs data was obtained from the JAEA Database for Radioactive Substance Monitoring Data (https://emdb.jaea.go.jp/emdb/en/). The $^{129}I/^{137}Cs$ activity ratio after June 2011 was calculated from the ^{129}I concentration observed by Suzuki et al. (2013) and this study and ^{137}Cs concentration observed by Oikawa et al. (2013) and Kaeriyama et al. (2014) (see Table S3 for details). Analysis of ^{129}I in seawater of this study followed the method of Suzuki et al. (2013). Horizontal arrows indicate the level before the accident. Dotted line in Fig. (c) indicates the mean $^{129}I/^{137}Cs$ activity ratio in sediment in 2011. Vertical lines indicate the boundary of the year.

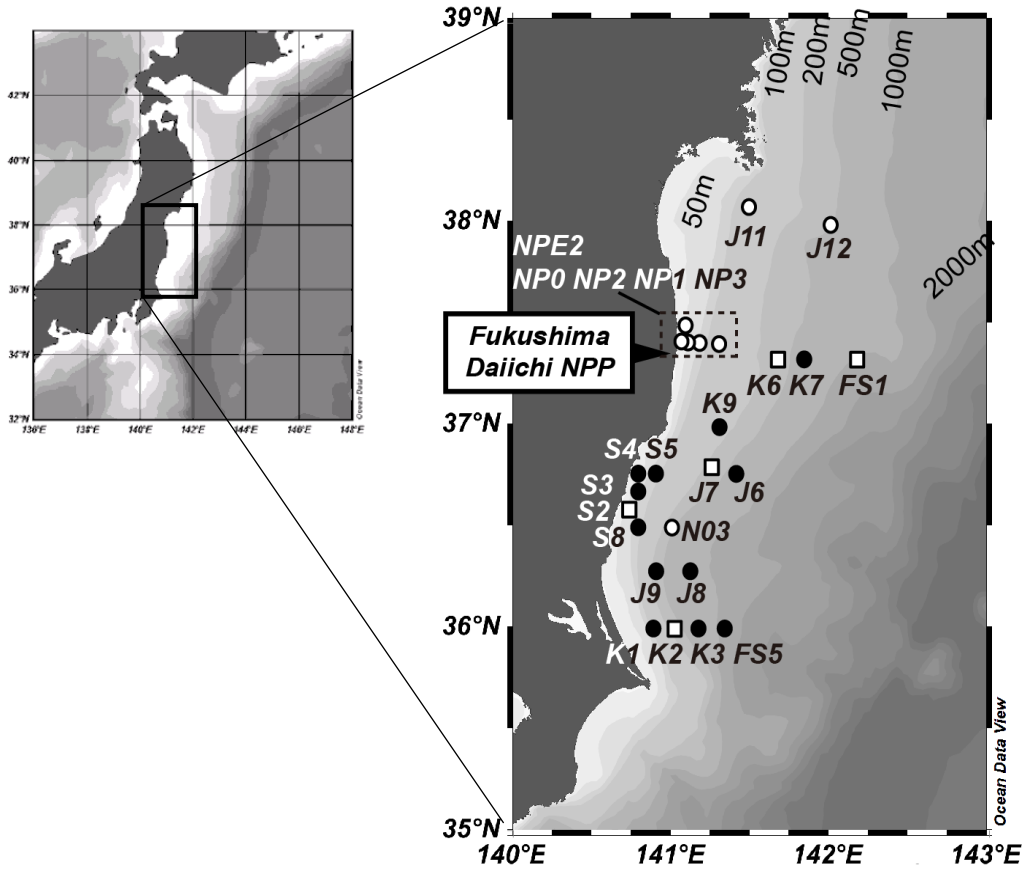

784

785

786 **Figure 1**

787

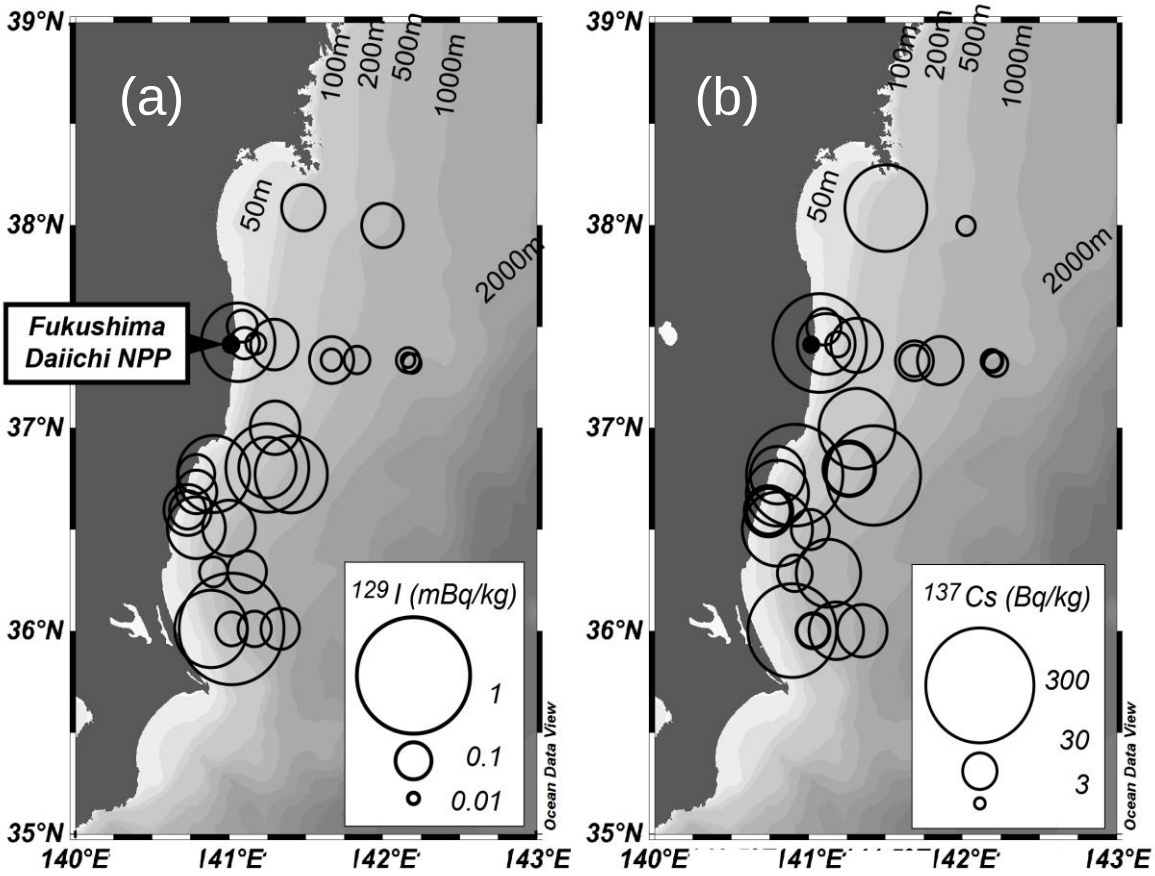

788

789 **Figure 2**

790

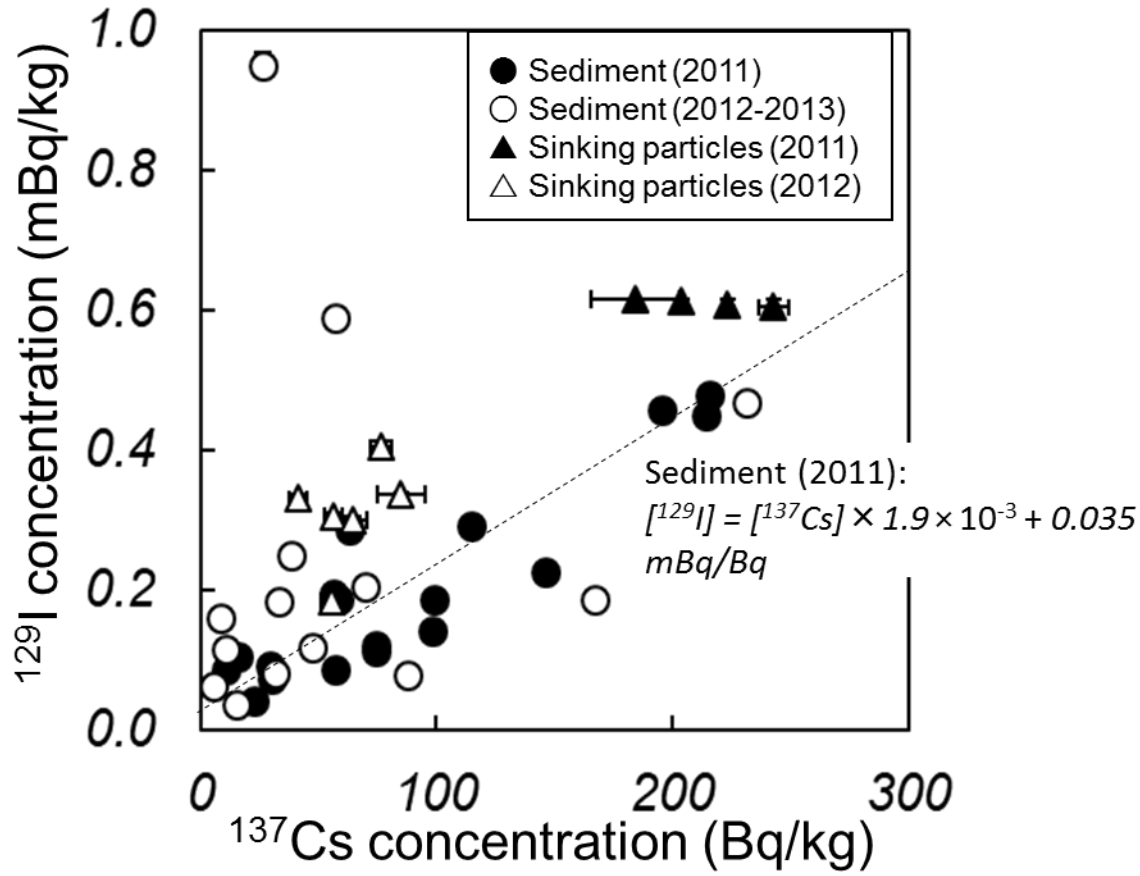

791

792 **Figure 3**

793

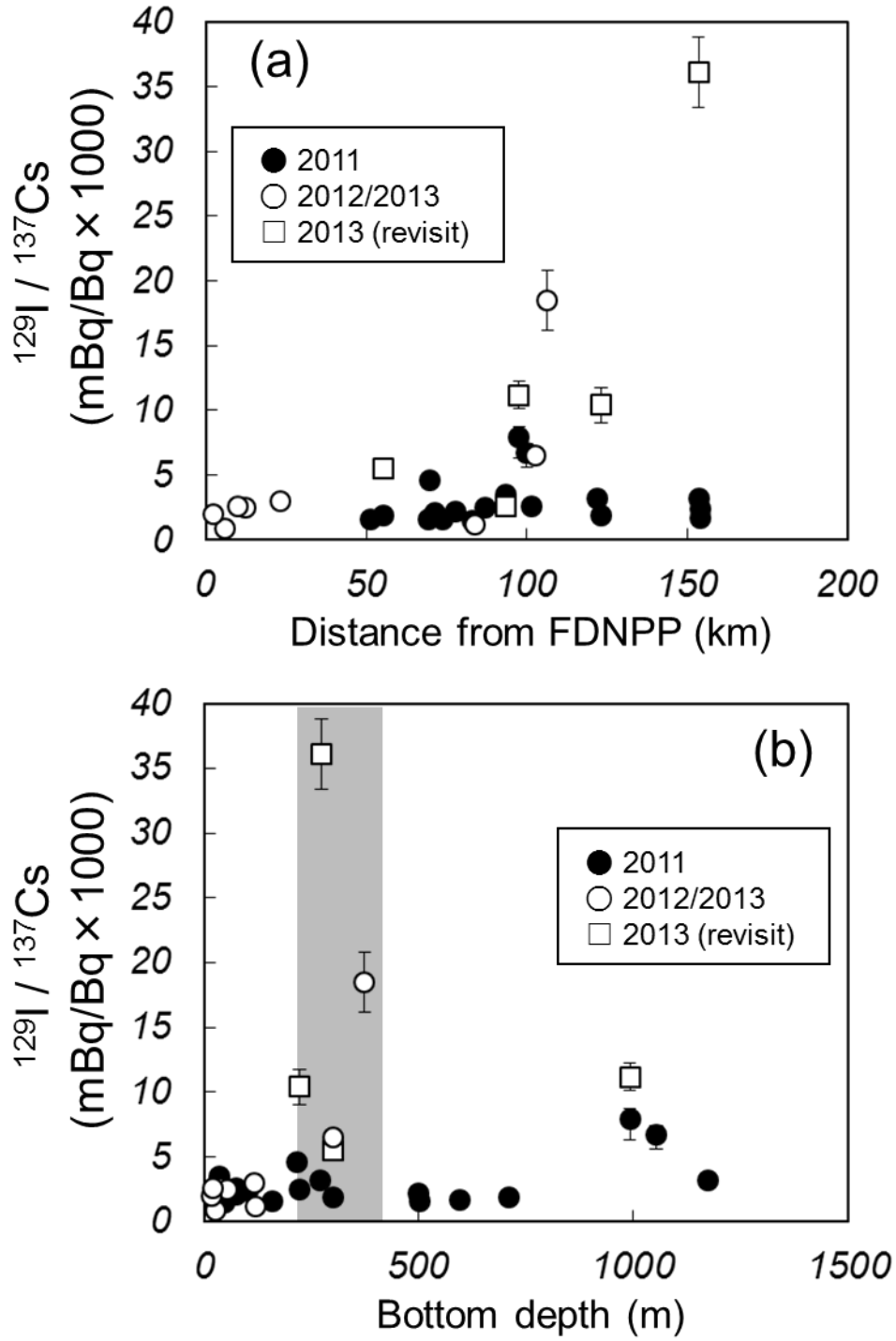

794

795 **Figure 4**

796

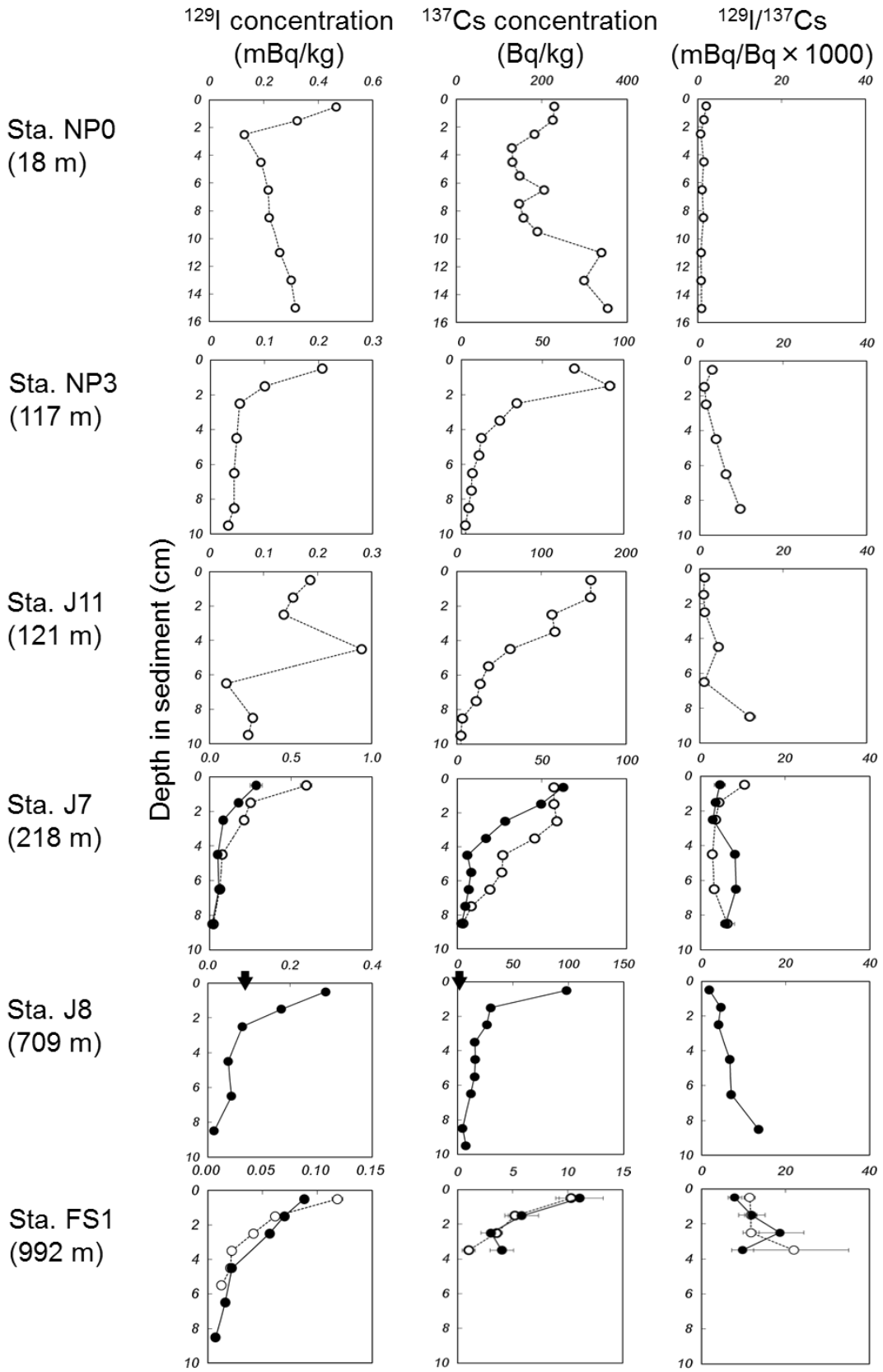

797

798 **Figure 5**

799

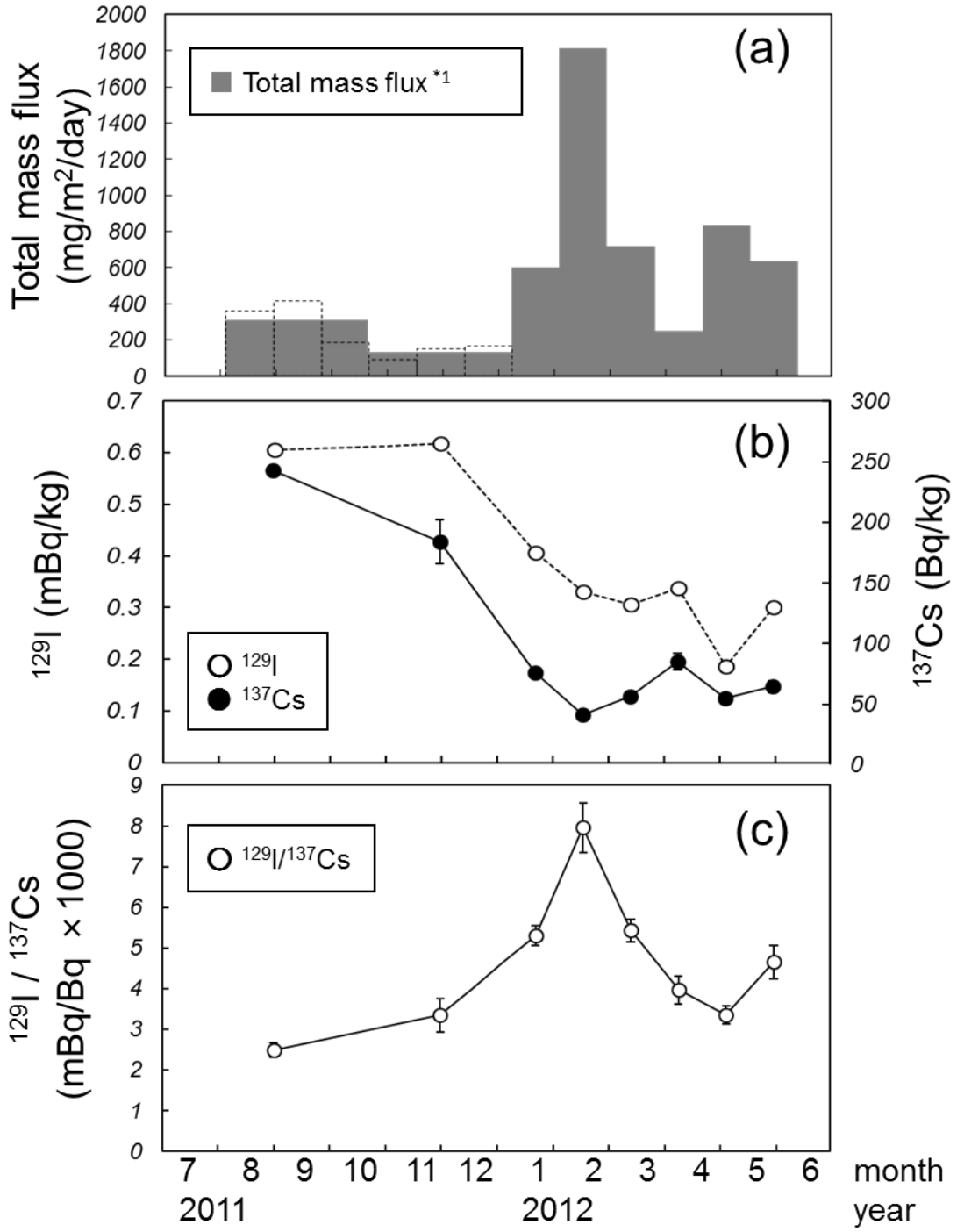

800

801 **Figure 6**

802

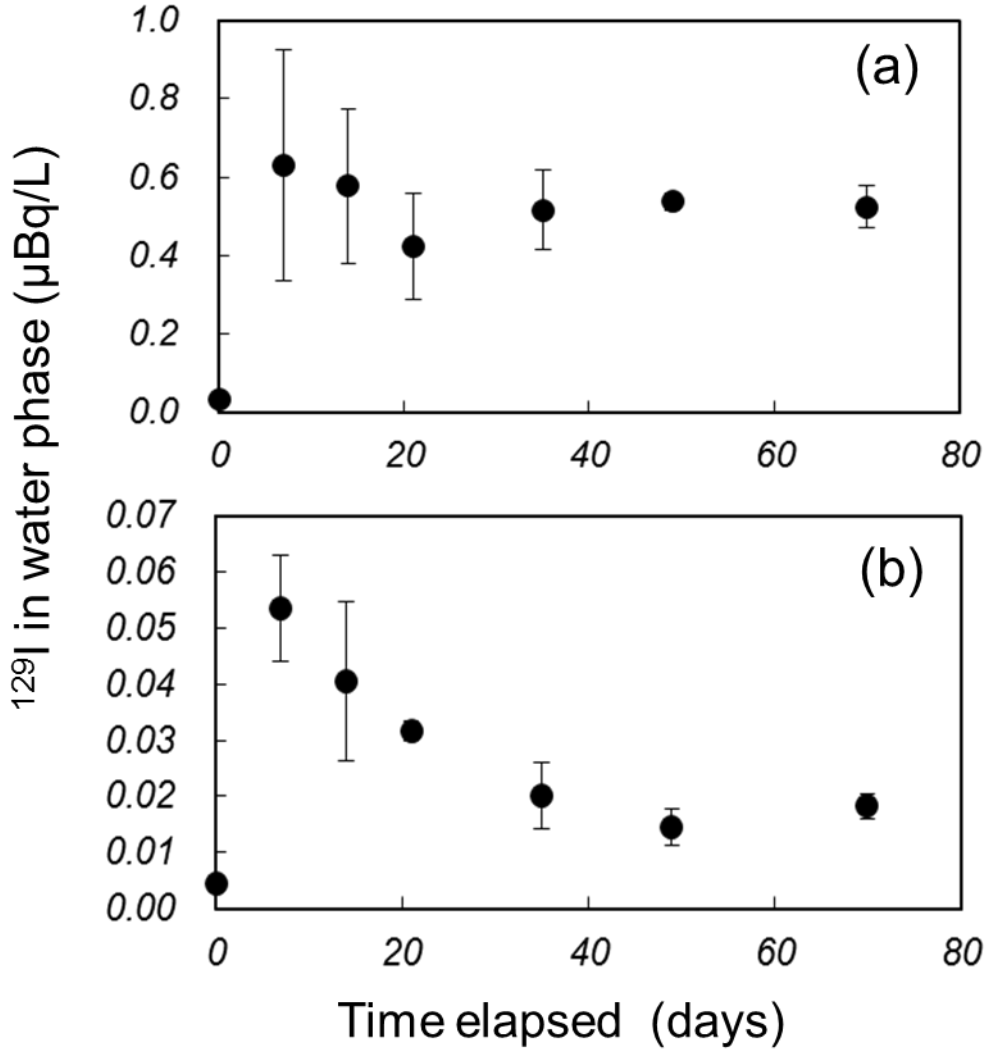

803

804 **Figure 7**

805

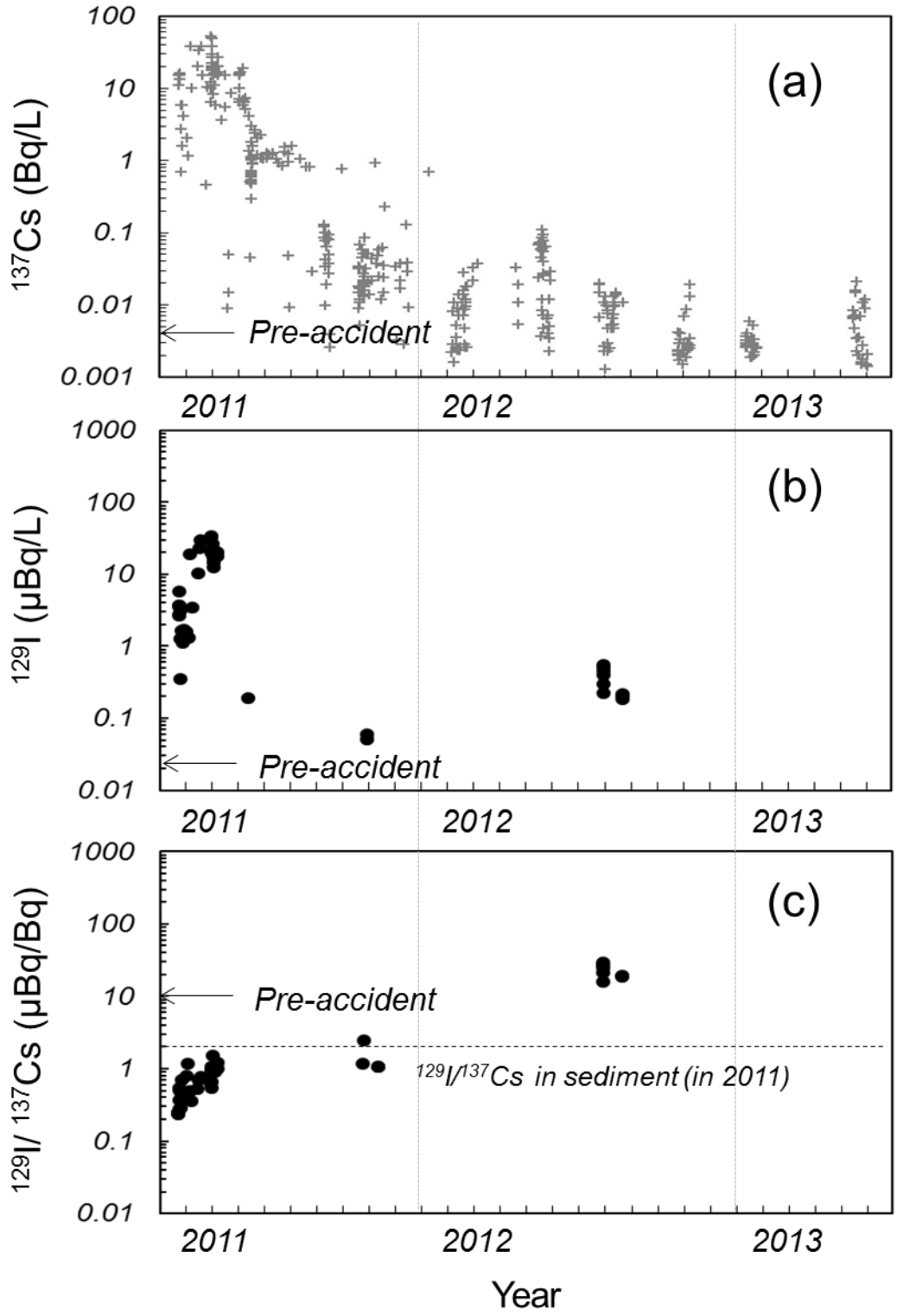

806

807 **Figure 8**

808